The Brookhaven $(g-2)_\mu$ Measurement

D.W. Hertzog[g], H.N. Brown[b], G. Bunce[b], R.M. Carey[a], P. Cushman[h], G.T. Danby[b], P.T. Debevec[g], H. Deng[l], W. Deninger[g], S.K. Dhawan[l], V.P. Druzhinin[i], L. Duong[h], W. Earle[a], E. Efstathiadis[a], F.J.M. Farley[l], G.V. Fedotovich[i], S. Giron[h], F. Gray[g], M. Grosse Perdekamp[l], A. Grossmann[e], U. Haeberlen[f], M. Hare[a], E.S. Hazen[a], V.W. Hughes[l], M. Iwasaki[k], K. Jungmann[e], D. Kawall[l], M. Kawamura[k], B.I. Khazin[i], J. Kindem[h], F. Krienen[a], I. Kronkvist[h], R. Larsen[b], Y.Y. Lee[b], I. Logashenko[i], R. McNabb[h], W. Meng[b], J.-L. Mi[b], J.P. Miller[a], W.M. Morse[b], C.J.G. Onderwater[g], Y. Orlov[c], C. Pai[b], C. Polly[g], J. Pretz[l], R. Prigl[b], G. zu Putlitz[e], S.I. Redin[l], O. Rind[a], B.L. Roberts[a], N. Ryskulov[i], R. Sanders[b], S. Sedykh[g], Y.K. Semertzidis[b], S. Serednyakov[i], Yu.M. Shatunov[i], E. Solodov[i], M. Sossong[g], A. Steinmetz[l], L.R. Sulak[a], C. Timmermans[h], A. Trofimov[a], D. Urner[g], D. Warburton[b], D. Winn[d], Q. Xu[b], A. Yamamoto[j], D. Zimmerman[h]

[a] *Department of Physics, Boston University*
[b] *Brookhaven National Laboratory*
[c] *Newman Laboratory, Cornell University*
[d] *Physics Department, Fairfield University*
[e] *Physikalisches Institut der Universität Heidelberg, Germany*
[f] *MPI für Med. Forschung, Heidelberg, Germany*
[g] *Department of Physics, University of Illinois at Urbana-Champaign*
[h] *Department of Physics, University of Minnesota*
[i] *Budker Institute of Nuclear Physics, Novosibirsk, Russia*
[j] *KEK, Japan*
[k] *Tokyo Institute of Technology, Tokyo, Japan*
[l] *Department of Physics, Yale University*

A new assault on the muon's anomalous magnetic moment has begun with a vigorous effort by the Brookhaven E821 collaboration. The present group has refined the design used in a series of successful CERN experiments in order to lower the systematic uncertainties. Consequently it will be possible to take advantage of the greatly increased muon flux provided for at the AGS. Several novel techniques are employed, of which the most significant is a direct muon injection scheme. Upon reaching the goal of the experiment, comparison with theory will offer sensitive tests of both the electroweak corrections and physics beyond the Standard Model. At the time of this Symposium, data from the first engineering run has been analyzed, yielding a result whose precision and value are comparable to those generated by the last CERN effort.

1 Introduction

The gyromagnetic ratio, g, relates the magnetic moment of a charged particle to its intrinsic spin through the relation

$$\vec{\mu} = g\frac{e\hbar}{2mc}\frac{\vec{\sigma}}{2}. \tag{1}$$

For point-like, spin-1/2 Dirac particles, $g = 2$. That g is not exactly 2 indicates coupling to virtual fields. In 1947, Kusch and Foley [1] measured a tiny deviation of the electron's g-factor from 2 and later that year Schwinger was able to account for this so-called anomalous magnetic moment by considerations of the self-interaction of the electron in its own electromagnetic field. The anomaly, given as $a_e = \frac{(g-2)}{2} = \alpha/2\pi$, is approximately 1/800. Today, a_e has been measured [2] to 4 parts per billion and remains in agreement with QED, the most precise theory in physics. Unlike the electron, the muon's anomalous magnetic moment depends more sensitively on additional physics contributions such as hadronic and weak radiative loops.[a]

Brookhaven experiment E821 has recently been commisioned with the goal of measuring the muon's anomalous magnetic moment, a_μ, to a precision of 0.35 ppm (parts per million). In absolute numbers, this corresponds to $\Delta a_\mu = \pm 40 \times 10^{-11}$. The motivation for targeting this level of sensitivity is mainly to explore possible hitherto unknown couplings at very high mass scales. The expression that conveys this "test" is

$$a_\mu^{new} = (a_\mu^{expt.} - a_\mu^{theory}), \tag{2}$$

where the "theory" contributions include the known effects due to QED, the Weak Interaction (WI) and virtual hadronic production. Before discussing the experiment, we review the situation for the expected Standard Model (SM) component of the anomaly noting whether the individual contributions are known to 0.35 ppm. Later we include a brief discussion of what may be concluded if, at the end of the effort, experiment and SM theory do not agree.

2 Theoretical expectations

The currently understood SM contributions to a_μ are listed in Table 1. The largest effect is due to quantum electromagnetic corrections which are understood and tested because of the higher-precision measurements of the electron's anomalous magnetic moment. The QED contribution is identical for the muon

[a] these effects are present for electrons but are reduced by the factor $(\frac{m_\mu}{m_e})^2 \approx 40,000$ and are thus negligible.

except that the vacuum polarization terms are larger because of the muon's non-trivial mass. The most recent evaluation [3] includes estimates of terms up to tenth order. The uncertainty is significantly better than that needed for our effort.

The weak interaction contributes similar radiative corrections. Full WI calculations through second order have been completed recently by several groups.[4,5] A surprising result is the fact that the 2nd order term amounts to approximately 20% of the first-order contribution and reduces the weak-interaction effect to about 1.3 ppm. The uncertainty is negligible. Our experiment is designed to observe the electroweak effect.

The creation of hadronic vacuum polarization (HVP) loops has a significant effect on a_μ with a signal of approximately 60 ppm. Leading and next-to-leading terms are important as is an appropriate assignment of uncertainty on each of these. Unlike QED and the WI, hadronic effects cannot be calculated from first principles. However, the first-order HVP diagram is related to the R ratio by a well understood dispersion relation. $R(s)$ is the function describing the cross section ratio $\sigma(e^+e^- \rightarrow hadrons)/\sigma(e^+e^- \rightarrow \mu^+\mu^-)$. The subtlety involves accumulating data from many different experiments, performing proper error assignment, and applying appropriate relative normalizations. The bookkeeping involves choices and extrapolation as the worldwide data set does not yet span all regions with the desired sensitivity.

Four independent evaluations [6,7,8,9] result in positive contributions to a_μ of 60.6, 60.24, 60.26, and 59.61 ppm, respectively. Each has an error of approximately 1.3 ppm. Hadronic τ decay data provides a second technique for evaluating HVP contributions. The decay $\tau^- \rightarrow \nu_\tau + W^-_{virtual}$ with the virtual W^- forming physical hadronic final states, contains the same information as the R ratio, up to an s value corresponding to the τ mass. Alemany, Davier and Höcker,[9] evaluated the ALEPH data and used it to lower their estimated HVP uncertainty to 0.81 ppm. Additional considerations drawn from theory,[10] lead Davier and Höcker to a more aggresive error of 0.64 ppm. Pushing the uncertainty lower requires additional data which is being provided now from the new CMD-2 experiment, very soon from the BES spectrometer, and eventually from an effort at DAPHNE.

Hadronic "light-on-light" is a more problematic second-order effect. The evaluation of this diagram is model dependent and has stimulated two major efforts and much discussion. The involved groups [11,12] now agree that the effect corresponds to a reduction in a_μ by 0.68 ± 0.13 ppm. The second-order (non "light-on-light") terms represent an additional 0.86 ppm reduction to a_μ. The estimate has been made by two groups [6,13] who agree on the details. The quoted uncertainty is negligible.

Table 1: Standard Model Contributions to a_μ.

Source	a_μ	Relative Precision
QED	$165847.06(2) \times 10^{-9}$	± 0.016 ppm
WEAK	$1.51(4) \times 10^{-9}$	± 0.03 ppm
HADRONIC	$67.71(77) \times 10^{-9}$	± 0.66 ppm
TOTAL	$1165916.28(77) \times 10^{-9}$	± 0.66 ppm

The net hadronic contribution continues to evolve. We expect the uncertainty on it to be near our goal of 0.35 ppm in a few years. The reader is cautioned that the number quoted in Table 1 may be adjusted. It is arrived at by using the most ambitious Davier and Höcker calculation for the HVP term together with the second-order computation by Krause and the light-on-light value from Hayakawa and Kinoshita.

3 Generic (g − 2) and E821 specifics

3.1 Overview

The measurement of the magnetic moment of a particle typically involves observation of the precession frequency of its spin vector when it is placed in a known magnetic field. Polarized particles are introduced into a magnetic channel and later the advancement of their spin vectors is evaluated. For weakly decaying particles, parity violation couples the particle's spin direction to the momenta of its emitted decay products. This correlation permits a measurement of the advancement of the spin in the field. For the muon's anomalous magnetic moment, relativistic polarized muons are introduced into a storage ring having a very pure vertical dipole magnetic field. As a muon undergoes cyclotron motion around the ring, its spin direction advances with respect to its momentum vector and eventually laps it. The lapping, or "difference" frequency is proportional to $(g-2)$.

Four key features conspire to enable an extrodinarily precise determination. The description of our experiment which follows is organized to follow these key points: (1) Pion decay provides an intense source of polarized muons; (2) The muon precession frequency is proportional to $(g-2)$ and not to g; (3) For a particular muon momentum, the spin precession is not affected by the electric "holding" field used for vertical containment; (4) The muon's spin direction is correlated to its decay products. These features were exploited in a remarkable series of experiments at CERN over the past several decades leading to a precision of 7.3 ppm for a_μ.[14] Excellent reviews exist.[15] Our experiment is built upon many of these same principles but features several new ideas, the most important of which is direct muon injection which has been installed for the 1998 run.

3.2 Polarized Muon Source

A 400-fold increse in statistics is required to improve on the last CERN effort by a factor of 20. To acheive this, the increased AGS proton intensities (above 40×10^{12} protons per pulse) are used to produce pions which are transported along a 116 m secondary beam line to a muon storage ring. Polarized muons result from the weak $\pi \to \mu\nu$ decay. The most energetic muons in this decay are emitted in the direction of the pion momentum and are highly polarized longitudinally. The pion beam line can deliver either muons or pions into the storage ring; for 1997, eight bursts of up to 10^8 particles were delivered every 2.6 seconds. The entrance to the storage ring is provided by a field-free "door" through the back steel yoke. A superconducting inflector magnet [16] cancels the storage ring field and permits the beam to enter nearly tangent and directly adjacent to the ring's circular storage volume.

To shift an entering particle's orbit to be commensurate with one within the storage volume requires a transverse momentum impulse of approximately 1%. This occurs in either of two modes. In pion injection (1997 run condition), muons are "accidentally" kicked onto a stable orbit with a probability of approximately 2×10^{-5} following direct injection of a pion into the ring. This pion enters the ring, turns about half way around and decays in a manner to place a forward-going muon of nearly the same momentum onto a stored orbit. Most of the pions instead create havoc by traversing the electromagnetic calorimeters or by striking the magnet steel. Hadronic interactions lead to a large number of secondary neutrons which eventually thermalize and are captured. The gammas which follow can produce light in the PMTs well after, and in addition to, the tremendous prompt "flash". For this reason, all phototubes are disabled for up to 100 μs in order to let the background from the flash settle down. A major new feature of E821 is a muon kicker magnet. This permits direct muon injection into the ring by providing the necessary transverse momentum impulse to the muon bunch during its first two trips around the ring. A test in 1997 indicates that this will lower the background by a factor of 50. Calculations estimate the number of stored muons will be increased by a factor of at least 10.

3.3 Precession Frequency

Positive muons loaded into the storage ring exhibit a circular (or helical) motion with a characteristic cyclotron frequency given by $\vec{\omega_c} = -\frac{e\vec{B}}{mc\gamma}$. Their spin vectors precess according to

$$\vec{\omega_s} = -\left[1 + \gamma\left(\frac{(g-2)}{2}\right)\right]\frac{e\vec{B}}{mc\gamma} \tag{3}$$

which is the Larmor frequency modified by the Thomas term.

The difference between Eq. (3) and the cyclotron frequency yields the difference frequency

$$\vec{\omega}_a = -a_\mu \frac{e\vec{B}}{mc} \tag{4}$$

where a_μ has been substituted for $(g-2)/2$. This important expression contains three key points. First, no relativistic γ factor appears; the spread in muon momenta does not need to be kept to less than a ppm[b]. Second, as pointed our earlier, ω_a is proportional to $(g-2)$. Finally, the main quantities which determine a_μ are ω_a and the average magnetic field; both must be measured to comparable precision since each enters the expression linearly. In practice, the ratio ω_a/ω_p is measured, where ω_p is the proton NMR freqency acquired in the same magnetic field. The link from this ratio to a final absolute result is bridged by the μ_μ/μ_p ratio which is known from hyperfine muonium transitions to 0.15 ppm.[17]

The new 14.1 m diameter superferric muon storage ring [18] at Brookhaven is designed to produce a highly uniform and stable magnetic field. The cross-sectional profile of the magnet structure is that of the letter "C" with the open side facing inward. This enables electrons from muon decay to spiral in to a detector system located on the inside of the ring. Within the "C" a muon storage volume is defined by collimaters to have a 9 cm diameter circular cross section. The yoke and pole pieces are made of semi-continuous segments of iron and steel respectively and the 1.45 T field is energized by three superconducting coils. An aggressive shimming effort has resulted in an integrated inhomegeneity in the integrated field of less than 1 ppm for the 1998 run and beyond.

3.4 Magic Gamma

Vertical containment of the muons is provided by four electric quadrupoles. They are placed symmetrically around the storage ring volume yet inside the

[b]In fact, $\Delta P/P$ for the muons is about 0.5%.

vacuum chambers. Normally, the muon spin would be affected by the presence of a static electric field following the more complete expression for the difference frequency when both a magnetic and electric field are present,

$$\vec{\omega}_a = -\frac{e}{mc}\left[a_\mu \vec{B} - \left(a_\mu - \frac{1}{\gamma^2 - 1}\right)\vec{\beta} \times \vec{E}\right]. \tag{5}$$

At a gamma of 29.3 the second term above vanishes and the precession is entirely due to the magnetic field. This last fact determines the desired muon momentum of 3.094 GeV/c. In Eq. (5), $\vec{B}$ represents the average magnetic field seen by the muons prior to their decay. To obtain this quantity, the field strength must be known precisely everywhere in the storage volume and the muon orbits must be predictable.

To accomplish the former, a system of fixed and movable NMR probes is used. These probes establish the magnetic field in units of the proton precession frequency over the entire storage volume and provide a system to monitor it continuously.[19] A unique feature is a moveable "trolley" which carries 17 NMR probes and enters the muon storage volume from an adjacent garage in order to travel inside the ring. A continuous 3D field-strength profile is built approximately daily throughout the run from information gathered during such trolley runs. Short term changes are monitored and corrected for by the use of 366 fixed probes located symmetrically around the ring in positions both above and below the muon vacuum chamber. The overall system is designed to produce a field map with a 0.1 ppm absolute uncertainty.

The muon orbit is convoluted with the field map to obtain the average magnetic field. The average orbit can be obtained from calculations assuming a phase-space distribution. This was done for the 1997 data and was justified by measurements of the muon momentum distribution. When the muon beam is introduced into the storage ring (even with pion injection), it arrives as a pulse train with a length characterized by a FWHM of approximately 50 ns. The bunch requires 149 ns to circle the ring. Due to the distribution in initial momenta of the muons, the particles debunch over time and the ring eventually can be considered to be uniformly populated. The initial bunch rotation frequency as well as the rate of the debunching is measured in one of the detector stations. The information is used to determine the average muon momentum and the distribution in momenta. Measurements match Monte Carlo calculations when we assume a phase space occupancy of the ring.

In the future, direct determination of the muon distribution will be made using an electron "traceback" system. Four straw drift chambers are placed at one location on the inside of the ring. Decay electrons which curl inside due to their lower momenta have a chance of passing through all four chambers. For such events, an arc is followed back into the ring to approximate the location where the parent muon decayed. A profile of the muon distribution is developed from an ensemble of such events. This system was tested and performed well in the 1997 run.

3.5 Access to the Muon Spin

The parity violating weak muon decay, $\mu^+ \to e^+\nu_e\bar{\nu}_\mu$, results in the most energetic electrons[c] being emitted in the direction of the muon spin. The higher-energy decay electrons (as determined in the muon's rest frame) are boosted to appreciable momenta in the lab frame. These electrons tend to "remember" the muon spin whereas lower-energy electrons do not. An electromagnetic calorimeter (EM) system consisting of 24 individual stations located symmetrically around the ring just to the inside of the muon storage volume, intercepts the electrons which are spiralling inward. It measures electron energy and arrival time. The ideal functional form describing the distribution of arrival times is

$$N(t) = N_0 e^{-t/\tau}[1 + A(E)\cos\omega_a t + \phi(E)] \tag{6}$$

where $A(E)$ is an energy-dependent asymmetry whose value is determined by the threshold for defining just what is a "high-energy" electron. For electrons above 1.8 GeV, A is approximately 0.4.

The 24 electromagnetic calorimeters [20] are made of a matrix of lead and scintillating fibers (Pb/SciFi). Each monolithic Pb/SciFi block presents a 14×22.5 cm cross sectional area to the entering electrons and is 15 radiation lengths deep (15 cm). The measured resolution is approximately $10 - 12\%\sqrt{E(\mathrm{GeV})}$ The fibers run radially and are read out by four R1828 or R3489 2″ photomultiplier tubes positioned near the floor to avoid line-of-site with the incoming beam and to remove them from proximity to the magnetic field. Lightguides transport the scintillator light from quadrants of the Pb/SciFi block to the individual PMTs. For electrons above a preset threshold, the summed analog signal is recorded by a custom 400 MHz waveform digitizer.

Electrons from muon decay spiral inward and strike the side face of a calorimeter module (i.e., they enter normal to the fiber direction). To avoid electron preshowering while exiting the vacuum chamber, a novel scalloped design is used. Upstream of each EM station, the inner vacuum chamber wall flairs gently toward the inside of the storage ring so that decay electrons

[c] at present, μ^+ and therefore "positrons" is correct; however, we will repeat the measurements with μ^- so the generic "electron" is used in the text.

exiting the storage volume encounter no material until just prior to entering the calorimeter station itself. With this design, and the excellent intrinsic resolution of the detectors, the theoretical maximum asymmetry contained in Eq. (6) is acheived.

The time-dilated lifetime of muons in the ring is 64 μs. Our electronics system is designed to collect data for nearly $600 \mu s$ following injection. A critical concern is any energy or time drift in the measurement system between early and late times following injection. A nitrogen laser (337 nm, 300 ps pulses) is used to strobe all detectors at preset times. Analysis of the time and energy determination of the laser pulses, compared to reference detectors outside of the ring, enables stringent tests of the system stability.

4 1997 Run Results

At the time of this Symposium, the E821 collaboration was finishing the analysis of approximately 170 hours of comissioning data based on pion injection running. An example of the quality of the signal is shown in Figure 1. It represents a sample of the nearly 11 million decay positrons recorded. A particular feature of this plot is the high asymmetry value which greatly exceeds that seen at CERN for the reasons quoted earlier. The details of the analysis of this data are described in Carey *et al.* [21] The new result of $a_\mu^{E821} = 1165925(15) \times 10^{-9}$ can be represented in terms of Eq. (2) by

$$a_\mu^{new} = (a_\mu^{E821} - a_\mu^{SM}) = (8.9 \pm 15.0) \times 10^{-9}$$

Combining E821 with the past CERN numbers yields $a_\mu^{new} = (7.1 \pm 7.2) \times 10^{-9}$. Obviously, the commisioning run has served mainly to prove that systems are working and that most of the components are in place. In 1998 and beyond, the introduction of the direct muon injection scheme will launch E821 into a new era. The goal of a combined statistical and systematic error at the 0.35 ppm level conjures up considerations of what this might test if experiment differs from SM theory by several standard deviations.

5 What if? Beyond the Standard Model

In the review of the theory for the muon's $(g-2)$ factor by Kinoshita and Marciano, a final section details new physics sensitivity.[3] Particular items to note include muon substructure, W boson compositeness, and certain models of supersymmetry. We briefly consider the latter two.

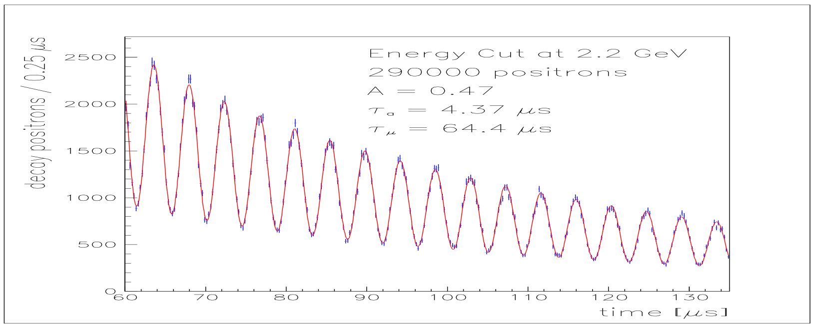

Figure 1: A sample of the data from the 1997 run. The evident oscillatory structure on top of the exponential carries the precession frequency which is proportional to $(g-2)$.

The magnetic moment of the W is expressed as $\mu_W = \frac{e}{2m_W}(1+\kappa+\lambda)$ and the relation to a_μ is found in the relevant contribution to the muon anomaly which is

$$a_\mu(\kappa,\lambda) = \frac{G_F m_\mu^2}{4\sqrt{2}\pi^2}\left[(\kappa-1)\ln\frac{\Lambda^2}{m_W^2} - \frac{\lambda}{3}\right]. \tag{7}$$

For a point-like W, $\kappa = 1$ and $\lambda = 0$. The sensitivity of E821, at the 2σ level then tests the g factor of the W to a precision of $\Delta(\frac{g_W-2}{2}) \approx 0.04$ which is substantially better than can be done at LEP 2.

At this Symposium, Chattopadhyah [22] described the particular sensitivity of the muon's anomalous magnetic moment to supergravity based grand unification models. The supersymmetric diagrams feature chargino-sneutrino loops and neutralino-smuon loops in first order and look topologically very much like the weak interaction diagrams. A very large effect on a_μ exists for large $\tan\beta$, where $\tan\beta$ is the ratio of Higgs vacuum expectation values. This fact was recognized earlier by Lopez, Nanopoulos and Wang [23] who calculated an a_μ contribution versus gluino mass for different assumptions on $\tan\beta$ (and on the top quark mass which was unmeasured at the time). In the Chattopadhyay and Nath (CN) version, additional parameters exist. After accounting for relations between parameters the model is described by the two mass scales m_0 and m_{gluino}, the top quark A parameter, and $\tan\beta$. An unknown sign for the parameter μ_0 introduces two sets of results for positive and negative assumptions, however the magnitude is fixed. A sample of this calculation is shown in Figure 2. The contours represent the 95% C.L. limit if the SM value agrees

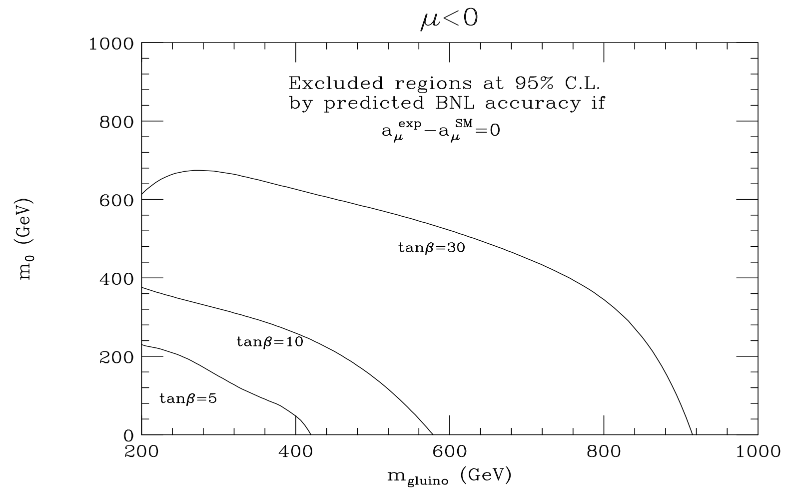

Figure 2: Contours of excluded regions from the Chattopadhyah and Nath Sugra Model based on hypothetical future $(g-2)$ experiment and SM agreement to 0.35 ppm. Excluded regions at the 95% C.L are below the contours for given $\tan\beta$ values.

with the final experimental result with a combined uncertainty of 0.35 ppm. For this scenario, the CN model excludes m_{gluino} and m_0 masses below 600 GeV for $\tan\beta \approx 30$, and below 400 and 200 GeV, respectively, for $\tan\beta \approx 10$. These mass scales are quite high compared to direct accelerator searches and to other indirect tests. Naturally, the reverse is true. For SUSY masses in this range, a large effect on a_μ can be expected.

6 Summary

The E821 collaboration has begun a new measurement of the muon's anomalous magnetic moment. The goal of a final precision at or below the 0.35 ppm limit appears to be attainable based on what we have seen in our first engineering run. At this level, new physics will be tested for particles which interact with the muon. This includes in particular supergravity-based supersymmetry for which our experiment now appears to be quite sensitive.

This research is supported by the United States Department of Energy, The National Science Foundation, the German Bundesminister für Bildung und Forschung, The Russian Ministry of Science and the US-Japan Agreement in High Energy Physics.

References

1. P. Kusch and H.M. Foley, *Phys. Rev.* **72**, 1256 (1947); *Phys. Rev.* **74**, 250 (1948).
2. R. van Dyke *et al.*, *Phys. Rev. Lett.* **59**, 26 (1987).
3. T. Kinoshita and W.J. Marciano in *Quantum Electrodynamics*, (Directions in High Energy Physics, Vol. 7) ed. T. Kinoshita, (World Scientific, Singapore, 1990), p. 419.
4. A. Czarnecki, B. Krause and W. Marciano, *Phys. Rev. Lett.* **76**, 3267 (1996); and *Phys. Rev.* D **52**, R2619 (1995).
5. G. Degrassi and G.F. Giudice, QED Logarithms in the Electroweak Corrections to the Muon Anomalous Magnetic Moment, hep-ph/9803384, March 1998.
6. T. Kinoshita, B. Nižić and Y. Okamoto, *Phys. Rev.* D **31**, 2108 (1985).
7. S. Eidelman and F. Jegerlehner, *Z. Phys.* C **67**, 585 (1985).
8. D.H. Brown and W.A. Worstell, *Phys. Rev.* D **54**, 3237 (1996).
9. R. Alemany, M. Davier and A. Höcker, *Eur. Phys. J.* C **2**, 123 (1998).
10. M. Davier and A. Höcker, *Phys. Lett.* B **419**, 419 (1998).
11. M. Hayakawa and T. Kinoshita, *Phys. Rev.* D **57**, 465 (1998).
12. J. Bijnens,E. Pallante and J. Prades, *Phys. Rev. Lett.* **75**, 1447 (1995); *Phys. Rev. Lett.* **75**, 3781 (1995), and *Nucl. Phys.* B **474**, 379 (1996).
13. B. Krause, *Phys. Lett.* B **390**, 392 (1997).
14. J. Bailey *et al.*, *Nucl. Phys.* B **150**, 1 (1979).
15. For example, see F.J.M. Farley and E. Picasso in *Quantum Electrodynamics*, (Directions in High Energy Physics, Vol. 7) ed. T. Kinoshita, (World Scientific, Singapore, 1990), p. 479.
16. F. Krienen, D. Loomba and W. Meng, *Nucl. Instrum. Methods* A **283**, 5 (1989).
17. Particle Data Group, *Phys. Rev.* D **54**, 1 (1996).
18. G. Danby *et al.*, to be submitted to *Nucl. Instrum. Methods* A.
19. R. Prigl *et al.*, *Nucl. Instrum. Methods* A **374**, 118 (1996).
20. S. Sedykh *et al.*, Proceedings of the 7th Int. Conf. on Calorimetry in High-Energy Physics (CALOR 97), Tucson, AZ, Nov. 9-14, 1997, (in press).
21. R.M. Carey *et al.*, submitted to *Phys. Rev. Lett.*, July 1998.
22. U. Chattopadhyay, these proceedings; and U. Chattopadhyay and P. Nath, *Phys. Rev.* D **53**, 1648 (1996).
23. J.L. Lopez, D.V. Nanopoulos and X. Wang, *Phys. Rev.* D **49**, 366 (1994).